



INTERNATIONAL JOURNAL OF MEDICAL

ARTS

Volume 7, Issue 9 (September 2025)



http://ijma.journals.ekb.eg/

P-ISSN: 2636-4174

E-ISSN: 2682-3780



Available online on Journal Website https://ijma.journals.ekb.eg

Main Subject [Radiology]



Original Article

Value of MDCT Angiography Using MIP and VRT Techniques for Determination of Tumor-Feeding Vessels in Transarterial Embolization of Hepatocellular Carcinoma

Mohamed S. Alwarraky; Rasha A. Aly; Muhammed A. Magdy; Maisara M. Rashed

Department of Interventional and Diagnostic Radiology, National Liver Institute, Menoufia University, Shebin Elkom, Menoufia, Egypt.

Abstract

Article information

Received: 29-05-2025

Accepted: 05-07-2025

DOI: 10.21608/ijma.2025.390390.2192

*Corresponding author

Email: drsasarashed@gmail.com

Citation: Alwarraky MS, Aly RA, Magdy MA, Rashed MM. Value of MDCT Angiography Using MIP and VRT Techniques for Determination of Tumor-Feeding Vessels in Transarterial Embolization of Hepatocellular Carcinoma. IJMA 2025 Sept; 7 [9]: 6108-6113. doi: 10.21608/ijma.2025.390390.2192.

Background: Transarterial chemoembolization [TACE] is a widely accepted palliative therapeutic approach for patients with intermediate-stage hepatocellular carcinoma [HCC].

Aim of The Study: This work aimed to detect the accuracy of maximum intensity projection [MIP] and volume rendering technique [VRT] techniques in identifying tumor-feeding arteries in patients undergoing TACE of hepatocellular carcinoma.

Patients and Methods: This was a retrospective study involved 34 patients with HCC who underwent TACE at the National Liver Institute, Menoufia University, Egypt. All patients underwent triphasic dynamic multidetector computed tomography [MDCT] prior to embolization. Arterial-phase images were reformatted and reconstructed using MIP and VRT techniques for the visualization and identification of tumor-feeding vessels. The findings were compared to digital subtraction angiography [DSA], which served as the reference standard. The diagnostic performance of both imaging techniques was statistically assessed in terms of accuracy.

Results: Substantial interobserver agreement was noted for both MIP and VRT [κ =0.705 and 0.671, respectively. Detection scores using MIP were elevated than VRT [mean 1.82 and 2.05 for observers 1 and 2, respectively, vs. mean 1.11 and 1.29 for observers 1 and 2, respectively; p < 0.001]. The accuracy of MIP and VRT in detecting tumor-feeding vessels, compared to DSA, was 68.89% and 42.22%, respectively

Conclusion: MDCTA using MIP technique is significantly accurate more than VR technique in the assessment of tumor-feeding arteries.

Keywords: Multidetector Computed Tomography Angiography; Maximum Intensity Projection; Volume Rendering Technique; Digital Subtraction Angiography; Hepatocellular Carcinoma; Transarterial chemoembolization.



This is an open-access article registered under the Creative Commons, ShareAlike 4.0 International license [CC BY-SA 4.0] [https://creativecommons.org/licenses/by-sa/4.0/legalcode.

INTRODUCTION

Hepatocellular carcinoma [HCC] continues to represent a significant global health challenge, ranking as the sixth most prevalent malignancy worldwide. In Egypt, it is the sixth most commonly diagnosed cancer among females and the second most frequent among males ^[1]. HCC carries a high mortality burden, accounting for over 250,000 deaths annually across the globe ^[2,3]. Epidemiological data reveal a notably high incidence in Asian countries, particularly China, where chronic infections with hepatitis B and C viruses are endemic and serve as the primary etiological factors ^[4]. Transarterial chemoembolization [TACE] has become a widely adopted palliative treatment for patients with intermediate-stage HCC who are not candidates for surgical resection or percutaneous ablation ^[3,5-6].

The success of TACE relies heavily on precise anatomical identification of the tumor-feeding arteries, along with detailed understanding of the vascular anatomy and appropriate delivery of chemoembolic agents ^[7]. Therefore, accurate preprocedural identification of the arterial supply to the tumor is essential.

Advancements in multidetector computed tomography [MDCT] and 3-dimensional [3D] imaging technology have significantly improved the visualization of vascular structures. MDCT angiography using maximum intensity projection [MIP] and volume-rendering technique [VRT] enables detection of small-caliber vessels and facilitates the creation of accurate vascular maps, which are critical for planning interventional procedures ^[8]. So, in our research we aimed to evaluate the role of MDCT angiography in assessing tumor-feeding vessels and to determine the diagnostic accuracy of MIP and VRT in their identification in HCC patients planned for TACE. It also aimed to assess the accuracy of hepatic arterial anatomy classification based on the Michels system.

PATIENTS AND METHODS

This is a Retrospective study carried out on 34 patients with HCC who underwent TACE in National Liver Institute, Menoufia, Egypt during the period from December 2023 to June 2024. The Ethical approval for this retrospective study was obtained from the Institutional Review Board [IRB] of the National Liver Institute, Menoufia University, under approval number 00699/2025. Prior to enrollment, all cases provided written informed consent.

Inclusion Criteria were 1] Diagnosed with HCC based on imaging [LI-RADS 5] or histopathology; 2] Underwent pre-procedural three phase dynamic CT covering the celiac and mesenteric arteries; 3] Underwent conventional angiography [DSA] during TACE procedure; 4] Complete imaging datasets available in Picture Archiving and Communication System [PACS]; 5] Complete clinical data available in Radiology Information System [RIS] and electronic medical records [EMR].

Exclusion Criteria were: 1] Poor quality or incomplete CT or DSA images; 2] Poor quality DSA study not showing the arterial feeders of HCC; 3] Missing or incomplete clinical documentation; 4] Received treatment by non-selective TACE procedure.

Reformation & reconstruction of Arterial phase of prior MDCT images was analyzed for determination of tumor-feeding vessels using MIP and volume-rendering technique [VRT]. Digital

subtraction angiography [DSA] served as the reference standard; accordingly, the identification of tumor-feeding vessels using MIP and VRT was compared with DSA findings, and the accuracy of each technique was calculated.

CT technique

A triphasic contrast-enhanced dynamic CT protocol, comprising arterial, portal venous, and delayed phases, was performed using a 128-slice MDCT scanner [Biograph mCT, Siemens Healthcare, Germany]. The scanning parameters are detailed in Table [1].

Table [1]: Scan parameters

Patient position	Supine with their arms above their head
Scout	Diaphragm to iliac crests
Scan direction	Cranio-caudal
Contrast injection consideration [Bolus	ROIat descending aorta
tracking]	Threshold100 HU
section thickness[mm]	2-5 mm
Pitch	1.75
contrast material	Non ionic contrast material 370
volume[ml]	1.5 ml\kg body weight
Iodine concentration[mg/ml]	370
Injection rate[ml/sec]	5 ml/sec
KV	130
MA	200
Collimation	6 mm
Arterial phase	35-45 sec post contrast injection
Portovenous phase	60-75 sec post contrast injection
Delayed phase	3 minutes

Transcatheter arterial embolization: Transarterial embolization with chemotherapy [TACE] or without chemotherapy was performed using a biplanar angiography system [ALLURA, PHILIPS]. Vascular access was obtained via the superficial femoral artery using the modified Seldinger technique. Selective DSA was conducted for the celiac artery, SMA, and CHA. Superselective catheterization of tumor-feeding vessels was then performed for precise embolization. Embolic agents included lipiodol, administered with or without doxorubicin, and gelatin sponge particles [gel foam].

Image analysis: Arterial phase images from MDCT were retrospectively transferred to a 3D workstation [IntelliSpace Portal, PHILIPS, IP: 192.168.116.189]. Tumor-feeding vessels were assessed using both MIP and VRT. The arterial phase was selected, and MIP mode was activated with a 3 mm slice thickness across axial, coronal, and sagittal planes. Window width and level were set to 600/250. Alternatively, the vascular analysis protocol was loaded, MIP mode was activated followed by bone removal then MIP images were saved [MIP coronal images]. VRT mode was activated; bones interfering with visualization were removed automatically or manually. Default opacity and color settings were applied, Then VR images were saved. Two abdominal radiologists with over five years of experience independently assessed the MIP and VRT images. Both readers were blinded to each other's interpretations as well as to the DSA findings, to minimize bias. Each radiologist independently evaluated the presence and number of tumor-feeding vessels and assessed hepatic arterial anatomy based on Michel's classification. In cases of disagreement between the two readers, a third senior interventional radiologist [with over 10 years of experience] reviewed the case to provide a consensus interpretation.

Tumor-feeding vessels were identified according to pre-defined imaging criteria: [1] their origin from hepatic arteries, [2] tortuous

or dilated morphology, [3] direct anatomical continuity with the tumor, [4] increased contrast enhancement, particularly in MIP reconstructions, [5] presence of a mesh-like neovascular network adjacent to the lesion, and [6] a visible "feeding vessel sign," defined as a single vessel leading directly to the tumor nodule or mass. These criteria were uniformly applied across MIP and VRT reconstructions to ensure standardized detection. DSA was used as the reference standard. Then comparison of tumor-feeding vessels on MIP and VRT with corresponding DSA images was performed by the radiologists. Cases were considered positive if vessels identified on MIP or VRT matched those on DSA; otherwise, negative.

Sample size calculation:

Sample size estimation was conducted based on previously reported data by **Kim** *et al.* ^[17]. indicating that the accuracy of Virtual Reality Technology [VRT] in assessing subsegmental tumor-feeding vessels compared with Digital Subtraction Angiography [DSA] was 22.2%, while the accuracy of Maximum Intensity Projection [MIP] was 77.8%. Using these proportions and setting the significance level at 0.05 and statistical power at 80%, the minimum required sample size was calculated using EpiCalc2000. The estimated sample size was 11 subjects per group, resulting in a total of 22 subjects needed for the study.

Statistical analysis:

Statistical analysis was conducted using SPSS version 27 [IBM©]. Normality was assessed by the Shapiro–Wilk test and histogram plots. Parametric quantitative data were expressed as mean \pm SD, while categorical variables were shown as frequencies and percentages. A two-tailed p-value < 0.05 was considered statistically significant. Interobserver agreement was evaluated using kappa statistics, interpreted as follows: <0 poor; 0.00–0.20 slight; 0.21–0.40 fair; 0.41–0.60 moderate; 0.61–0.80 substantial; 0.81–1.00 almost perfect agreement.

RESULTS

In this study, 75 patients were assessed for eligibility; 10 The study included 34 patients diagnosed with hepatocellular carcinoma [HCC], with a mean age of 64.82 ± 7.06 years [range: 48-77 years]. The majority were male [76.5%]. This demographic distribution aligns with established epidemiological patterns of HCC, which demonstrate a male predominance and peak incidence in older adults, particularly in regions with a high prevalence of chronic liver disease. Detailed demographic data are provided in **table [2].**

Most patients [82.4%] presented with a solitary hepatic lesion, with the right lobe being the predominant site of involvement [88.2%]. This is consistent with the anatomical and functional predominance of the right lobe in hepatic perfusion. The segmental distribution revealed a predominance in segments VI and VIII, each involved in approximately 29.4% of cases, indicating a concentration of tumor burden in segments with complex vascular supply [Table 3].

Most of the cohort [47.1%] had undergone at least one prior TACE session. Repeated embolization may contribute to altered hepatic arterial anatomy, including the development of collateral supply or vascular remodeling, which complicates feeder identification [Table 3].

DSA, serving as the reference standard, identified a total of 90 tumor-feeding vessels among the 34 patients. While 47.1% of patients had two feeders, an equal proportion demonstrated more than two, reflecting the highly vascular nature of intermediate-stage HCC [Table 4].

Anatomical evaluation of the hepatic artery, based on Michel's classification, revealed that 88.2% of patients exhibited the classic type I pattern. Type III and IV variants were identified in 5.9% of patients each. Notably, both MIP and VRT techniques demonstrated complete concordance with DSA in classifying hepatic arterial anatomy [accuracy = 100%] [Table 5].

In the identification of tumor-feeding vessels, MIP outperformed VRT with an accuracy of 68.89% compared to 42.22%, respectively. Interobserver agreement was substantial for both techniques [$\kappa = 0.705$ for MIP; $\kappa = 0.671$ for VRT]. The superior diagnostic yield of MIP may be attributed to its enhanced contrast resolution and ability to clearly delineate small-caliber vessels against surrounding hepatic parenchyma. VRT, while beneficial for spatial visualization, was more prone to overlapping structures, thereby limiting its utility in fine vascular discrimination [Table 6].

Table [2]: Demographic data of the studied patients

		N =34
Age [years]	Mean ±SD	64.82 ± 7.06
	Range	48-77
Sex	Male	26[76.47%]
	Female	8[23.52%]

 Table [3]: Characters and hepatic segmental distribution of the studied patients

N =34			
Number of lesions	One lesion	28[82.35%]	
	Two lesions	2[5.88%]	
	Three lesions	4[11.76%]	
Site of lesions	Right lobe	30[88.24%]	
	Left lobe	2[5.88%]	
	Bilobar	2[5.88%]	
Segments affected	III and V	2[5.88%]	
	VI	10[29.41%]	
	VII	4[11.76%]	
	VIII	10[29.41%]	
	VI \VII	2[5.88%]	
	IV a	2[5.88%]	
	V	2[5.88%]	
	VIII\V	2[5.88%]	
Previous interventions	One TACE session	16[47.05%]	
	Two TACE session	4[11.76%]	
	No	14[41.176%]	

TACE: Trans-catheter arterial embolization with chemotherapy.

Table [4]: The numbers of tumor feeding vessels assessed by DSA of the studied patients

No. of tu	mor feeding vessels	N =34	
DSA	One feeder	2[5.88%]	
	Two feeders	16[47.05%]	
	More than two feeders	16[47.05%]	

DSA: Digital Subtraction Angiography.

Table [5]: The type of hepatic supply [Michel's classification] assessed by DSA, MIP and VRT of the studied patients

Michel's classification	DSA	MIP	VRT	P value
Type I	30[88.24%]	30[88.24%]	30[88.24%]	1.00
Type III	2[5.88%]	2[5.88%]	2[5.88%]	1.00
Type IV	2[5.88%]	2[5.88%]	2[5.88%]	1.00

DSA: Digital Subtraction Angiography, MIP: Maximum intensity projection, VRT: Volume rendering technique.

Table [6]: Interobserver Agreement and Accuracy Of MIP And VRT In Detection of Tumor-Feeding Vessels Compared to DSA Findings of the Studied Lesions

DSA [n=90]	MIP	VRT	P value
- Positive	62	38	<0.001*
- Negative	28	52	
Kappa	0.705	0.671	
Accuracy	68.89%	42.22%	

^{*}Significant as P value≤0.05, DSA: Digital Subtraction Angiography, MIP: Maximum intensity projection, VRT: Volume rendering technique.

Case-I [Figure 1]: Male patient 72 years with segment IV previously managed HCC [*], coronal CT angiography with MIP Reconstruction [A], VR image [B] & DSA image [C] show replaced RHA [white arrow] from SMA with LHA [blue arrow] originates from LGA [Michel type IV]. In this case MIP image [A] matches with DSA image [C], with good depiction of tumor feeding vessels [Red arrow] and classified as positive.

Case-II [Figure 2]: Male patient 65 years with Right lobe segment VI HCC [Blue arrow], coronal CT angiography with MIP reconstruction [A], VR image [B]& DSA image [C] shows early bifurcation of CHA into RHA & LHA with GDA originates from LHA. In this case MIP image shows good depiction of tumor feeding vessels [yellow arrows] consistent with DSA image and classified as positive.

Case-III [Figure 3]: Female patient 71 years with previously embolized Right lobe segment VI HCC [blue arrow], coronal CT angiography with MIP reconstruction [A], VR image [B] & DSA image[c] shows Normal anatomy of HA. In this case MIP image, VR image match DSA image with good depiction of tumor feeding vessels [Red arrows].

Case IV [Figure 4]: Male patient 65 years with previously embolized Right lobe segment VIII HCC [black arrow] coronal CT angiography with MIP reconstruction [A], VR image [B] & DSA image[C] shows Replaced Right HA from SMA [Michel type III]. In this case MIP & VR images show good depiction of tumor feeding vessels [blue arrows] consistent with DSA images and classified as positive

Case V [Figure 5]: Male patient 48 years with previously managed Right lobe segment V HCC [blue arrow], coronal CT angiography with MIP reconstruction [A], VR image [B] & DSA image [C] show normal anatomy of HA. MIP image shows good depiction of tumor feeding vessels [yellow arrows] consistent with DSA image and classified as positive.

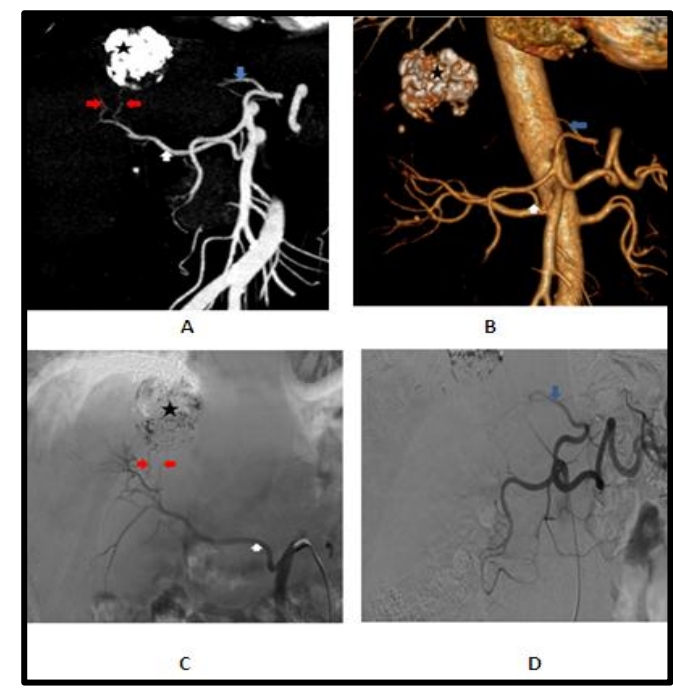


Figure [1]: Case -I

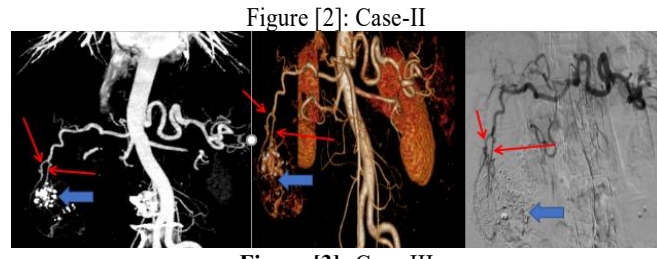


Figure [3]: Case-III

Figure [4]: Case-IV

Figure [5]: Case-V

DISCUSSION

HCC is the sixth most common cancer worldwide. For patients with intermediate-stage disease, TACE is considered the primary treatment. The procedure's efficacy depends on precise delivery into the arterial branches supplying the tumor, making accurate pre-treatment identification of these vessels essential. This requires a clear understanding of the CHA and its anatomical variants, as well as recognition of any extrahepatic branches that may supply the lesion—whether recruited spontaneously or following prior interventions such as surgery or TACE. As emphasized by **Cazejust and co-authors** [9], radiologists must actively identify and report these vessels on sectional imaging to ensure proper catheterization during the procedure.

DSA has traditionally been the standard imaging tool for identifying feeding arteries, including HA and ectopic sources. However, its invasive nature, high cost, and limited capacity to detect all relevant vessels restrict its use [10].

More recently, MDCT has been increasingly utilized in the evaluation of various vascular pathologies involving the head, thorax, coronary arteries, and abdomen. MDCT offers a comprehensive imaging modality that incorporates multiplanar reconstruction [MPR], curved planar reconstruction [CPR], MIP, and volume rendering [VR]. This technique is regarded as a non-invasive alternative to DSA for visualizing hepatic and perihepatic vasculature, as well as for identifying tumor-feeding vessels prior to TACE. Based on previous study, the prevalence of hepatic anatomical variations is very common ranging from 20-50% [11].

In our research, we found that 30 patients [88.24%] had normal anatomy of the hepatic artery and only 4 patients [11.76%] had anatomical variants. While other studies such as **Abdelhamed** *et al.* ^[12] revealed that [72%] of cases had normal anatomy of the hepatic artery and only [28%] had anatomical variants. **Osman and Abdrabou** ^[13] and **Garg and co-authors** ^[14] reported that normal anatomy of the hepatic artery was presented in 74.2%, and 72% of cases respectively.

The most common variant in several studies based on Michel's classification is type III, which is found in 6-15.5% of cases [15].

In our research, we found that the most frequent variant was III and type IV equally presented in [5.88%] and [5.88%] of cases respectively. However, **Abdelhamed** *et al.* [12] found that the most frequent variant was type III presented in [12%] of cases. In addition, **Brasil and co-authors** [16] found that type III was the most common anatomical variant presented in 10%.

Our research exhibited that CT angiography was highly accurate in assessing and evaluating the anomalies in the hepatic artery compared to the outcomes of DSA; the accuracy

of MIP and VRT was 100%. While **Abdelhamed** *et al.* ^[12] & **Kim and co-authors** ^[17] stated that the accuracy of MIP and VRT for assessment of hepatic artery anomalies was 100% and 94% & 100% and 91% respectively.

Our research revealed that [47.05%] of 44 HCCs had two feeders, [47.05 %] of lesions had more than two feeders & [5.88 %] of lesions had single feeders. While **Abdelhamed** *et al.* reported that majority of lesions [70.6%] had single feeder arteries, [20.6%] lesions had two feeder arteries and only [8.8%] of lesions had more than two feeder arteries [12].

In addition, **Abdelsalam and co-authors** ^[18] reported that [35.1 %] of lesions had two feeder arteries, [24.6%] of lesions had more than two feeder arteries and [21.1%] of lesions had single feeder arteries.

Regarding the source of feeder arteries, we found that all feeders originate from hepatic branches with no extrahepatic supply. While **Abdelhamed** *et al.* stated that [96.9%] of feeder arteries were from branches of hepatic arteries and [3.1%] feeder arteries were extra-hepatic from right inferior phrenic artery left internal mammary artery [12].

In addition, **Miyayama and co-authors** ^[19] found that [1.9%] of detected feeder arteries were from inferior phrenic arteries.

Concerning the accuracy of CT angiography for assessment of feeding arteries of HCC compared to results of DSA, our research found that MIP had more accuracy than VRT in detecting the feeder arteries. MIP revealed 62 feeder arteries [68.89%] while VRT revealed only 38 feeder arteries [42.22%].

These findings match **Abdelhamed** *et al.* ^[12] who reported that the MIP had more accuracy than VRT in detecting the feeder arteries. MIP revealed 84 feeder arteries [87.5%] while VRT revealed only 23 feeder arteries [24%].

In addition, our results match **Kim and co-authors** who reported that the accuracy of MIP and VRT for detecting the feeder arteries of HCC was 77.8% and 22.2% respectively [17].

The superior performance of MIP in evaluating hepatic arterial anatomy is attributed to its high attenuation and strong contrast resolution of the HA. In contrast, VRT often results in visual overlap between the arteries, hepatic parenchyma, and surrounding structures, which may lead to misinterpretation. While VRT is useful for illustrating the spatial relationship between vasculature, soft tissues, muscle, and bone, MIP is more effective in delineating fine vascular structures, particularly small branches in organs such as the liver and kidney. In the current research, MIP achieved higher scores in the visual assessment of tumor-feeding vessels compared to VRT. MIP demonstrated clearer differentiation between the hepatic parenchyma and both the HA and HCC. This is due to its method of projecting the brightest voxels

within a volume, enhancing arterial contrast. On the other hand, VRT occasionally made it difficult to distinguish small intrahepatic vessels from the intensely enhanced parenchyma, even with proper parameter adjustment.

This study is subject to several limitations. The small sample size of only 34 patients restricts the statistical power of the findings and limits their generalizability to broader populations. A larger cohort would be necessary to validate the diagnostic performance of MIP and VRT techniques with greater confidence. The retrospective design inherently introduces potential biases, including selection bias and information bias, which may influence the results. These methodological limitations were not fully accounted for in the study and should be considered when interpreting the conclusions. Future prospective, multi-center studies with larger sample sizes are recommended to substantiate and expand upon these findings.

Conclusion: TACE remains the standard treatment for patients with intermediate-stage HCC, and its success is heavily dependent on precise anatomical mapping of the target vasculature. Therefore, evaluation of the HA anatomy and its variants using pre-procedural CT is essential. In this context, MDCT angiography with MIP has demonstrated high accuracy in identifying tumor-feeding arteries. Its application is expected to reduce procedure time, contrast agent usage, and radiation exposure during TACE.

Financial and Non-Financial Relationships and Activities of interest: None.

REFERENCES

- Torre LA, Siegel RL, Ward EM, Jemal A. Global Cancer Incidence and Mortality Rates and Trends--An Update. Cancer Epidemiol Biomarkers Prev. 2016 Jan; 25 [1]:16-27. doi: 10.1158/1055-9965.EPI-15-0578.
- Bruix J, Sherman M; American Association for the Study of Liver Diseases. Management of hepatocellular carcinoma: an update. Hepatology. 2011 Mar;53[3]:1020-2. doi: 10.1002/hep.24199.
- McGlynn KA, London WT. Epidemiology and natural history of hepatocellular carcinoma. Best Pract Res Clin Gastroenterol. 2005 Feb;19[1]:3-23. doi: 10.1016/j.bpg.2004.10.004.
- Taura N, Hamasaki K, Nakao K, Ichikawa T, Nishimura D, Goto T, et al. Aging of patients with hepatitis C virus-associated hepatocellular carcinoma: long-term trends in Japan. Oncol Rep. 2006 Oct;16[4]:837-43. PMID: 16969503.
- Kawano Y, Sasaki A, Kai S, Endo Y, Iwaki K, Uchida H, et al. Short- and long-term outcomes after hepatic resection for hepatocellular carcinoma with concomitant esophageal varices in patients with cirrhosis. Ann Surg Oncol. 2008 Jun;15[6]:1670-6. doi: 10.1245/s10434-008-9880-7.
- Xiao EH, Hu GD, Li JQ, Huang JF. [Transcatheter arterial chemoembolization in the treatment of hepatocellular carcinoma]. Zhonghua Zhong Liu Za Zhi. 2005 Aug;27[8]:478-82. Chinese. PMID: 16188145.

- Lim HS, Jeong YY, Kang HK, Kim JK, Park JG. Imaging features of hepatocellular carcinoma after transcatheter arterial chemoembolization and radiofrequency ablation. AJR Am J Roentgenol. 2006 Oct; 187 [4]: W341-9. doi: 10.2214/AJR.04.1932.
- Güven K, Acunaş B. Multidetector computed tomography angiography of the abdomen. Eur J Radiol. 2004 Oct;52[1]:44-55. doi: 10.1016/j.ejrad.2004.03.032.
- Cazejust J, Bessoud B, Colignon N, Garcia-Alba C, Planché O, Menu Y.
 Hepatocellular carcinoma vascularization: from the most
 common to the lesser known arteries. Diagn Interv Imaging.
 2014 Jan;95[1]:27-36. doi: 10.1016/j.diii.2013.04.015.
- Sacco R, Bertini M, Petruzzi P, Bertoni M, Bargellini I, Bresci G, et al. Clinical impact of selective transarterial chemoembolization on hepatocellular carcinoma: a cohort research. World journal of gastroenterology: WJG. 2009 Apr 21;15[15]:1843. doi: 10.3748/wjg.15.1843
- 11. Fonseca-Neto OCLD, Lima HCS, Rabelo P, Melo PSV, Amorim AG, Lacerda CM. ANATOMIC VARIATIONS OF HEPATIC ARTERY: A STUDY IN 479 LIVER TRANSPLANTATIONS. Arq Bras Cir Dig. 2017 Jan-Mar;30[1]:35-37. doi: 10.1590/0102-6720201700010010.
- Abdelhamed MS, Elsharawy FA, Youssef MA, Omar H. Comparative Research for Identification of Feeding Arteries of Hepatocellular Carcinoma by 3D Reformatted CT Angiography and Digital Subtraction Angiography during Transcatheter Arterial Chemoembolization [TACE]. Egy J Hospital Med. 2024 Apr 1;95. DOI: 10.21608/ejhm.2024.351022
- Osman AM, Abdrabou A. Celiac trunk and hepatic artery variants: A retrospective preliminary MSCT report among Egyptian patients. Egy J Radiol Nucl Med. 2016 Dec 1;47[4]:1451-8. doi: 10.1016/j.ejrnm.2016.09.011
- Garg S, Kumar KH, Sahni D, Yadav TD, Aggarwal A, Gupta T. Anatomy of the hepatic arteries and their extrahepatic branches in the human liver: A cadaveric study. Ann Anat. 2020 Jan;227: 151409. doi: 10.1016/j.aanat.2019.07.010.
- 15. Roma S, D'Amato D, Ranalli T, Nardone V, Pace C, Lenci I, et al. Vascular anomalies of the celiac trunk and implications in treatment of HCC with TACE. Description of a case and review of the literature. Radiol Case Rep. 2019 Aug 3;14[10]:1221-1227. doi: 10.1016/j.radcr.2019.07.011.
- 16. Brasil IRC, de Araujo IF, Lima AALA, Melo ELA, Esmeraldo RM. Computed tomography angiography study of variations of the celiac trunk and hepatic artery in 100 patients. Radiol Bras. 2018 Jan-Feb;51[1]:32-36. doi: 10.1590/0100-3984.2016.0179.
- 17. Kim I, Kim DJ, Kim KA, Yoon SW, Lee JT. Feasibility of MDCT angiography for determination of tumor-feeding vessels in chemoembolization of hepatocellular carcinoma. J Comput Assist Tomogr. 2014 Sep-Oct; 38 [5]: 742-6. doi: 10.1097/RCT.0000000000000103.
- 18. Abdelsalam H, Emara DM, Hassouna EM. The efficacy of TACE; how can automated feeder software help? Egy J Radiol Nucl Med. 2022 Feb 15;53[1]:43. doi:10.1186/s43055-022-00720-4
- Miyayama S, Yamashiro M, Sugimori N, Ikeda R, Okimura K, Sakuragawa N. Outcomes of Patients with Hepatocellular Carcinoma Treated with Conventional Transarterial Chemoembolization Using Guidance Software. J Vasc Interv Radiol. 2019 Jan;30[1]:10-18. doi: 10.1016/j.jvir.2018.08.009.





INTERNATIONAL JOURNAL OF MEDICAL

ARTS

Volume 7, Issue 9 (September 2025)



http://ijma.journals.ekb.eg/

P-ISSN: 2636-4174

E-ISSN: 2682-3780